Supporting Information

Dispersible Conjugated Polymer Nanoparticles as Bio-Interface Materials for Label free Bacteria Detection

Nada Elgiddawy[1, 2], Shiwei Ren[3], Abderrahim Yassar[3], Alain Louis-Joseph[4], Hélène Sauriat-Dorizon[1], Waleed M.A. El Rouby[5], Ahmed O. El-Gendy[6], Ahmed A. Farghali[5], Hafsa Korri-Youssoufi[1*]

[1] Université Paris-Saclay, CNRS, Institut de Chimie Moléculaire et des Matériaux d'Orsay (ICMMO), ECBB, Bât 420, 2 Rue du Doyen Georges Poitou, 91400, Orsay, France

[2]Department of Biotechnology and Life Sciences, Faculty of Postgraduate Studies for Advanced Sciences (PSAS), Beni-Suef University, Beni-Suef, 62 511, Egypt.

[3] LPICM, CNRS, Ecole Polytechnique, Institut Polytechnique de Paris, route de Saclay, 91128 Palaiseau, France

[4] PMC, CNRS, UMR 7643, Institut Polytechnique de Paris, route de Saclay, 91128 Palaiseau, France.

[5] Materials Science and Nanotechnology Department, Faculty of Postgraduate Studies for Advanced Sciences (PSAS), Beni-Suef University, Beni-Suef, 62 511, Egypt

[6] Microbiology and Immunology Department, Faculty of Pharmacy, Beni-Suef University, Beni-Suef, Egypt

Corresponding Author: Hafsa Korri-Youssoufi
Email:hafsa.korri-youssoufi@universite-paris-saclay.fr

Table of contents:

SI.1 Materials and Methods

Materials

Lauria broth (LB) medium, phosphate buffer saline, Rogosa and Sharpe (MRS) were purchased from Sigma Aldrich Co. The other reagents and solvents: triethylene glycol monomethyl ether, 3-bromothiophene, i-PrMgCl, 2,5-dibromo-3-hexylthiophene, [1,3-bis(diphenylphosphino)propane]-dichloronickel (II), Ni(dppp)Cl_2, N-bromosuccinimide, THF, $CDCl_3$, methanol-d4, etc. were purchased from commercial suppliers and used as received without any further purification.

SI.1.1 Instrumentation

The nuclear magnetic resonance (NMR) spectra were collected on a Bruker ARX 400 NMR spectrometer with deuterated solvents and tetramethylsilane (δ = 0 ppm) as the internal standard. For Nuclear Overhauser Spectroscopy (NOESY) experiments, the pulse program used was a 2D homonuclear correlation via dipolar coupling. Dipolar coupling may be due to dipolar coupling NOE or chemical exchange. NOESY acquisitions were performed on 8 scan with a mixing time of 150 ms and a relaxation delay of 1s. The self-assembling behavior and micelle formation were characterized by ^1H and NOESY NMR using deuterated THF-d8 , $CDCl_3$ as solvent and CD_3OD as a selective non-solvent. Ultraviolet-visible (UV-vis) absorption spectra were carried out on a Carry spectrophotometer. FT-IR spectroscopy measurements were carried out using FT-IR spectrophotometer Bruker equipped with attenuated total reflection (Pike) unit and MCT detector. The average size of micelles was measured by dynamic light scattering (DLS). Static water contact angle measurements to characterize the surface wettability were carried out using CAM-200 equipment. This involves the placement of microliter sized droplets of water on a surface of polymer modified glass substrate and measure the angle formed at the boundary of the droplet. Optical microscopy characterizations were performed using a Nikon E600POL microscope. SEM observations were recorded using a JEOL-2100F Scanning electron microscope and an internal charge coupled device (CCD) camera. TEM image is recorded using (JEOL JEM-2100) multipurpose, 200 kV analytical electron microscope.

GPC was performed with a two-column ViscoGel mixed bed from Viscotek (7.8 × 300 mm, type GMHH r-H). This mixed bed was mounted on a device equipped with a refractive index detector (Waters 410). The injected volume of sample solution was equal to 50 μL. HPLC

pump and THF as eluent and flow rate of 1mL/ml was used and a volume of 50µl of solution of P3HT-b-P3TEG (1mg/ml). The calibration range corresponded to polystyrene standards.

SI.1.2 Synthesis of P3HT-*b*-P3TEGT

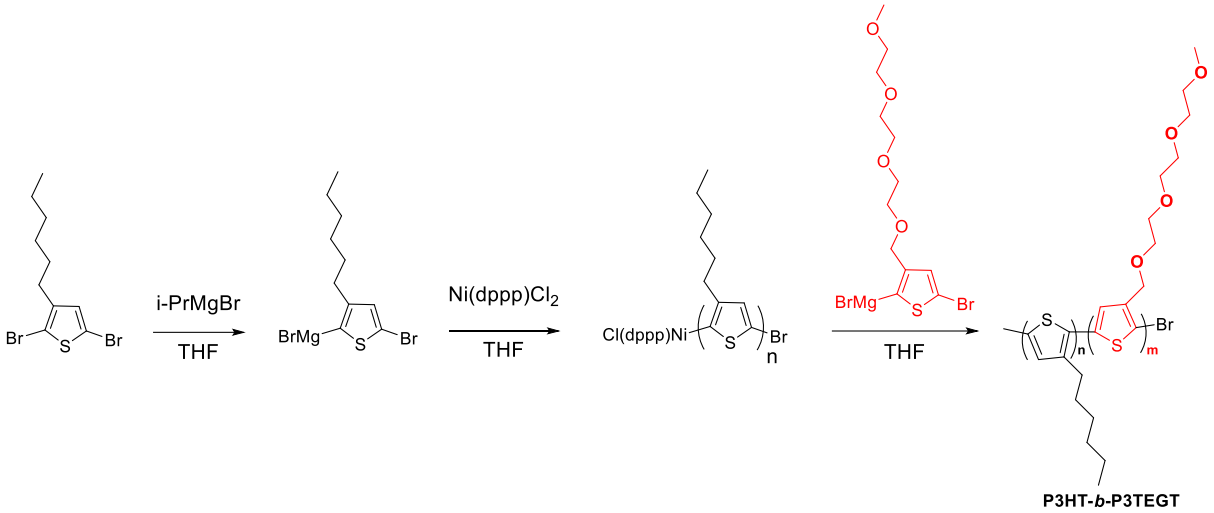

Scheme S1. Synthesis of P3HT-*b*-P3TEGT

2,5-Dibromo-3-hexylthiophene (0.5 mL, 2.4 mmol) was dissolved in 40 mL of anhydrous THF in a 100 mL three-necked flame-dried round-bottom flask under argon. After cooling at 0° C, freshly prepared molar solution of i-PrMgBr (THF, 2.5 mL, 2.5 mmol) was added via a syringe. The reaction was maintained at RT under stirring for 2 h. Then Ni(dppp)Cl_2 13,6 mg (0,024 mmol, 0,01 mol%/monomers) was added in one portion. The mixture was stirred at room temperature for 2 h. In a separate flask, 2,5-dibromo-3-(2-(2-(2-methoxyethoxy)ethoxy)ethoxy)methylthiophene (1 g, 2.4 mmol) was dissolved in 20 mL of anhydrous THF under argon. i-PrMgBr (1 M in THF, 2.6 mL, 2.6 mmol) was then added via a syringe and the mixture was stirred at RT for 2 h. The obtained Grignard solution was then cannulated into the flask containing the P3HT macroiniator, and copolymerized for overnight at RT. The reaction was then quenched by pouring into 300 mL of methanol. The copolymer was isolated by centrifugation (5 000 rpm) and purified by sequential Soxhlet extractions using methanol, hexane, and chloroform, respectively. The chloroform fraction was dried to yield the final copolymer, with a moderate molecular weight, as a deep purple solid (0.28 g, 29%).

SI.1.3 Self-assembly studies and nanomicelle formations

For nanomicelle formations, typically 0.05 mg or (1mg, 5 mg) of P3HT-b-P3TEGT was firstly dissolved in 1 mL of THF. 100 µL of this solution was injected into 1 mL of mixture of methanol and THF, followed immediately by gentle mixing. The ratio of methanol in the mixture (methanol/THF) was varied from 30% to 100%, with the following volume 30% MeOH (300µL MeOH / 700µl THF); 50% MeOH (500µl MeOH, 500 µL THF); 70% MeOH (700µL MeOH, 300µL THF) and 100% MeOH (1mL MeOH).

The effect of the ratio of methanol on the nanomicelle formation was studied by UV-Visible and NMR measurements. UV-Visible was performed with low concentration of 0.05 mg/mL of the copolymer. For ^{1}H NMR studies of self-assembly were performed with high concentration due to sensitivity of the instrument. 5.0 mg of P3HT-b-P3TEGT copolymer was dissolved in 1 mL of $CDCl_3$ and then to 0.5 mL of this solution, anhydrous merhanol-D4 was added gradually with various ratio 0.1 mL MeOH; 0.15 mL MeOH; 0.2 mL MeOH; 0.25 mL MeOH, 0.3 mL MeOH and 0.4 mL MeOH.

DLS measurements were performed to follow the stability and the formation of the nanomicelles using three concentrations of the P3HT-*b*-P3TEGT (0.05 mg/mL, 1 mg/mL and 5 mg/mL) in various volume ratios of methanol, 30, 50, 70 and 100%.

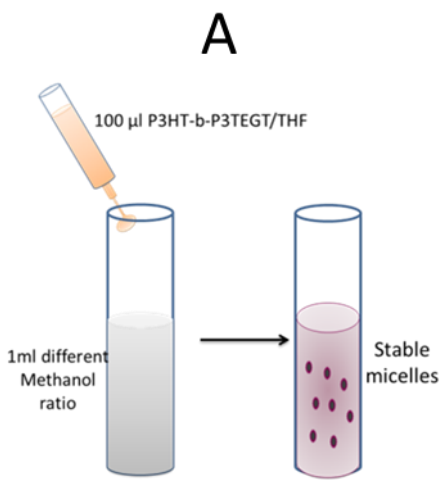

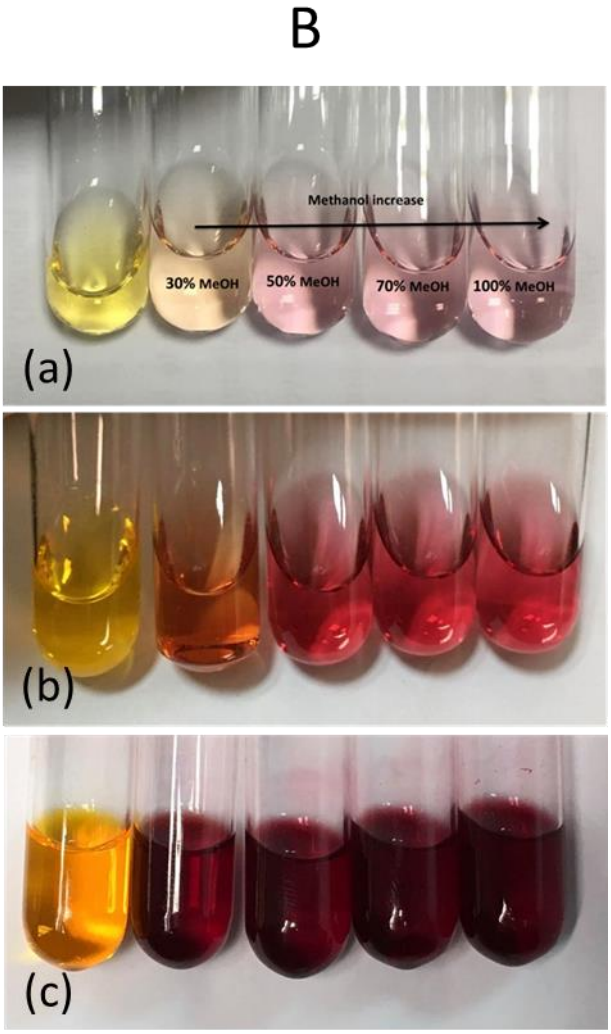

Scheme S2: (A) Schematic view of the approach for the preparation process of P3HT-*b*-P3TEGT nanomicelles, (B) Photograph of THF solution of nanomicelles with various ratios added of methanol and various concentrations of the P3HT-*b*-P3TEGT 0.05 mg/mL (a), 1 mg/mL (b) and 5 mg/mL(c).

SI. 1.4 Bio-interface fabrication and preparation of mannose modified nanomicelles

For the preparation of mannose decorated P3HT-*b*-P3TEGT nanomicelles, 1.0 mg of P3HT-*b*-P3TEGT copolymer was dissolved in 1 mL of THF and stirred at 60 °C under dark conditions for 2 h, the resulting solution of copolymer was mixed with mannose dissolved in anhydrous methanol (5 mg/mL), and stirred at room temperature (scheme S3). Three various ratios of P3HT-*b*-P3TEGT: mannose was studied by varying volume ratio of the solution THF/methanol (50/50, 66/33, and 75/25) to achieve nanomicelles with different weight ratios of P3HT-*b*-P3TEGT to mannose (1:5, 2:5 and 3:5), denoted as (P1M5, P2M5, P3M5). The obtained emulsion of nanomicelles was used directly to modify GCE by a simple drop cast

procedure. This was done by casting of 8 µL of blend of nanomicelle solutions P3HT-*b*-P3TEGT/mannose on the surface of GCE and dried at 50 ^{0}C for 2 h. The film was then rinsed with distilled water to remove the excess of untrapped mannose. For TEM sample preparation, 100 µL of 1mg/mL of P3HT-b-P3TEGT solutions in THF were dropwised into 1 mL of anhydrous methanol and the same into 1 mL of anhydrous methanol containing 5 mg mannose. Resulting solutions were drop casted on Cu grid and dried at ambient temperature.

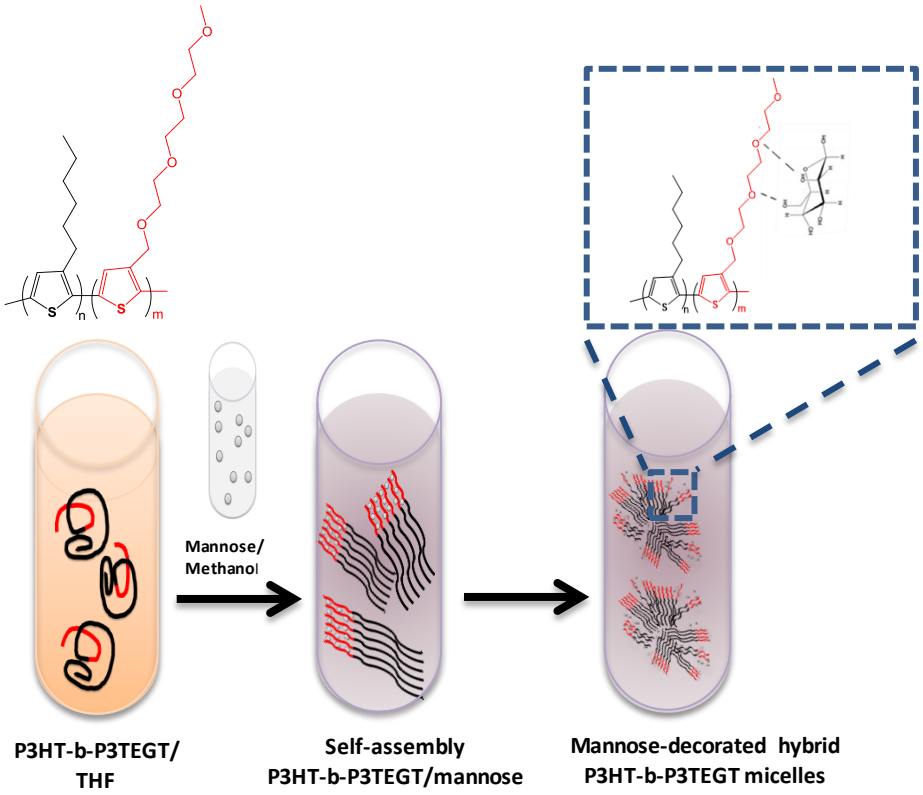

Scheme S3: schematic representation of self-assembly and nanomicelles formation of mannose decorated P3HT-*b*-P3TEGT.

SI. 2 Results and discussion

SI. 2.1 Synthesis of P3HT-*b*-P3TEGT and characterizations

SI.2.1.1 NMR characterizations

^{1}H-NMR spectrum of P3HT-*b*-P3TEGT and its peak assignment were performed to characterize molecular structure of the copolymer and diblock formation (Figure S1a). It is evident that, for all of the protons in the P3HT-*b*-P3TEGT, there are only two sets of signals observed in the spectrum. This is due to the highly symmetrical structure of P3HT-*b*-P3TEGT in which the proton of a particular position in each of the thiophene unit is under a chemically identical environment. The signals at 2.80 and 4.66 ppm are assigned to the protons of the

α−methylene units in the α−position of the thiophene ring of the P3HT block and the oxyethylene protons of the TEGT segment, respectively. In the aromatic region the block copolymer shows two singlets at 6.98 and 7.26 ppm corresponding to the aromatic proton of the thiophene ring of the P3HT (assigned Ha) and the P3TEGT block (assigned Hb) respectively. The peaks at 2.6 and 2.8 ppm corresponding to the α-CH_2 groups (assigned Hf) from hexyl chains have been used to determine the molecular weight distribution and regioregularity of P3HT. These peaks are assigned to the α-CH_2 groups on the terminal tail of 3-hexylthiophene units and the to all the α-CH_2 groups in the internal hexyl chains from the polymer, respectively. Therefore, the relative ratio of those two peaks provides the degree of polymerization hence the molecular weight of the polymer. From NMR analysis a degree of polymerization of P3HT block of ~ n=18-20 was estimated. The block length was estimated by the integration of ^{1}H NMR signal at 2.80 ppm assigned to methylene proton of the hexyl group (assigned Hf) and the singlet at 4.66 ppm of the oxymethylene proton next to the thiophene ring (assigned Hc). The P3HT-*b*-P3TEGT consists of 70 mol% of 3-hexyl-thiophene and 30 mol% of thiophene unit substituted with oxyethylene groups, which is very close to the feed ratio of the monomers used during the copolymerisation. ^{13}C NMR spectrum gives also detailed informations on the sequence structure of P3HT-*b*-P3TEG, Figure S1b. The molecular weights of the copolymer was estimated using gel permeation chromatography (GPC), M_n = 15 Kg/mol, D = 1.6, Figure S1c.

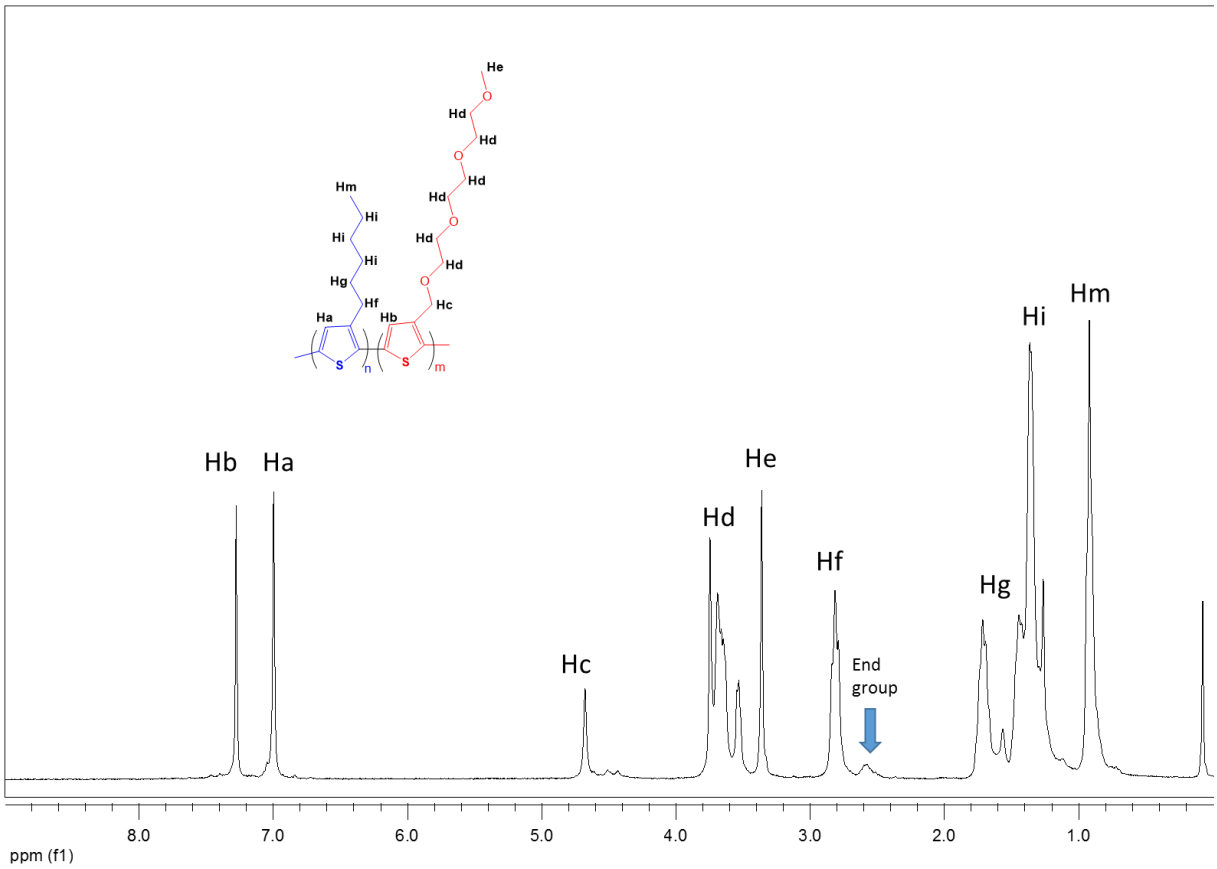

Figure S1a. ^{1}H-NMR spectrum of P3HT-*b*-P3TEGT diblock copolymer in $CDCl_3$

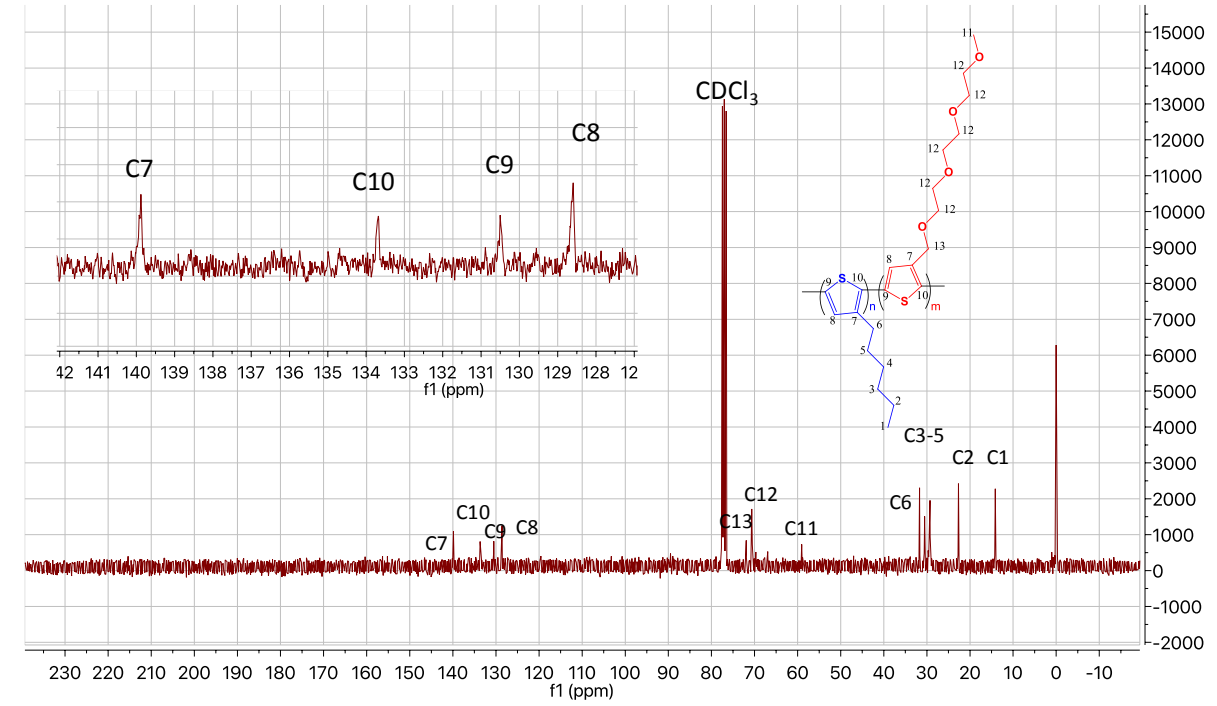

Figure S1b. ^{13}C-NMR spectrum of P3HT-*b*-P3TEGT diblock copolymer in $CDCl_3$

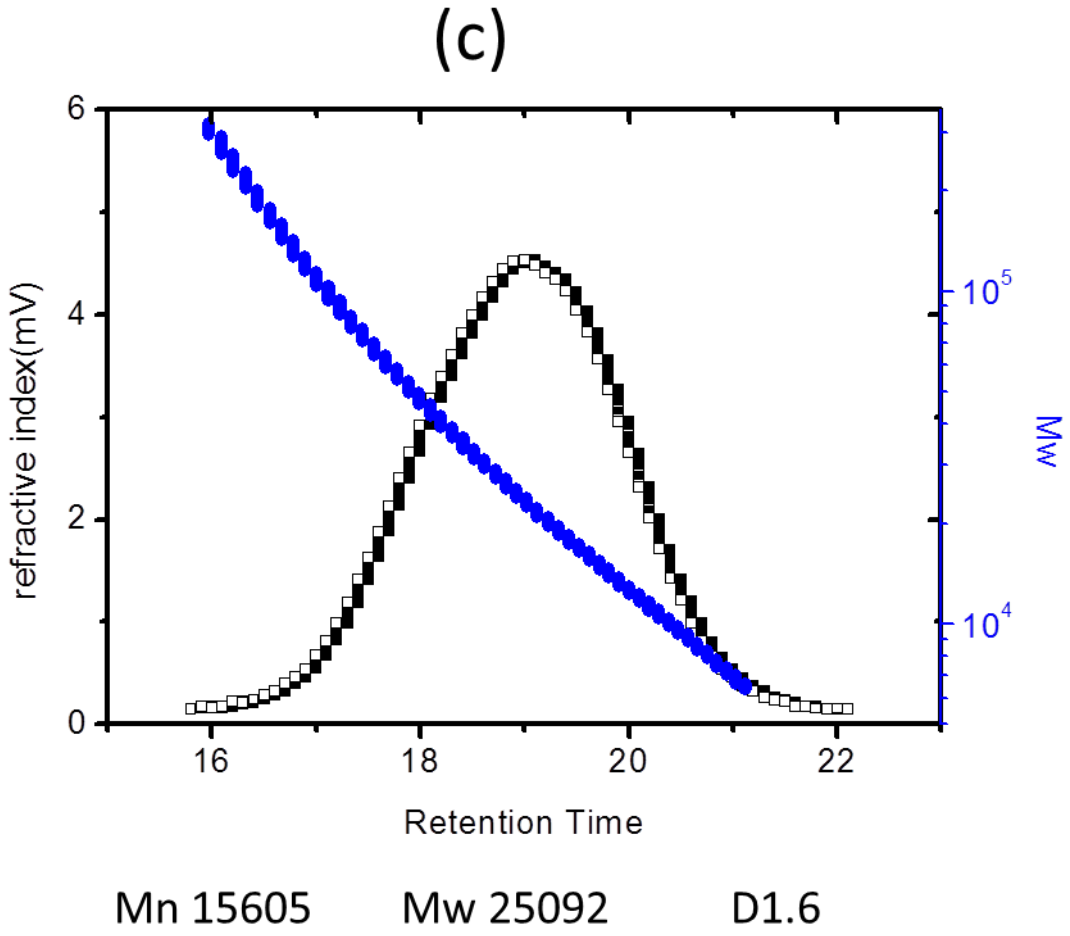

Figure S1c. A typical gel permeation chromatogram of P3HT-*b*-P3TEGT with calibration with polystyrene.

SI.2.1.2 FT-IR characterization

Figure S2 shows the FT-IR spectra of drop-casting film of P3HT-*b*-P3TEGT-nanoparticles. The spectrum shows the characteristic vibration bands related to the two blocks of copolymer, the C─H framework stretching at 2859 cm^{-1}, bending CH_2 and CH_3 at 1467 cm^{-1}, and at 1342 cm^{-1}, respectively. Stretching vibration band around 1460 cm^{-1} associated with a symmetric C=C ring, while the peak at 1507 cm^{-1} is related to an asymmetric C=C ring stretching vibration, as well as C–O–C asymmetric and symmetric stretching at 1103 cm^{-1} and at 960 cm^{-1}, respectively related to the oxyethylene chain.

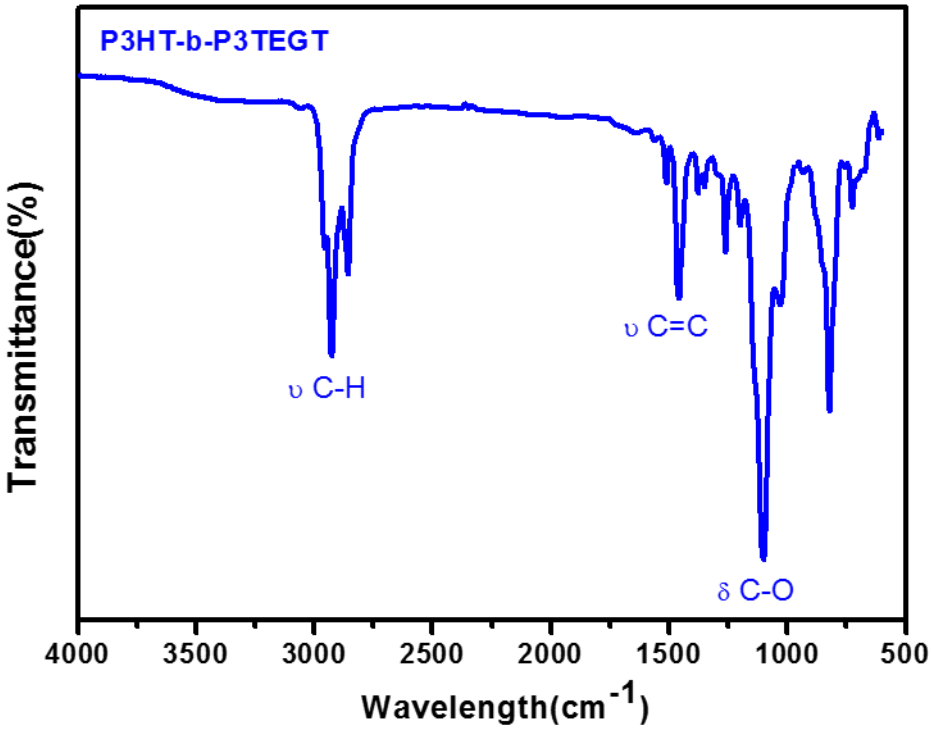

Figure S2. FT-IR spectra of drop-casting film of P3HT-*b*-P3TEGT-nanoparticles performed through ATR mode.

SI. 2.2. Nanomicelle characterization

SI.2.2.1 NMR characterization

The self-assembly and micellization behavior were observed in THF-d8 and THF-d8/methanol-d4 mixture (Figure S3). NMR results show no significant shift of copolymer proton but a decrease in intensity of peaks related to P3HT block as Ha and Hf which support clearly that the P3HT-*b*-P3TEGT self-assembled into polymeric core-shell nanomicelles with double-layer architecture formed by a hydrophobic P3HT block interior surrounded by a hydrophilic exterior PEGT block.

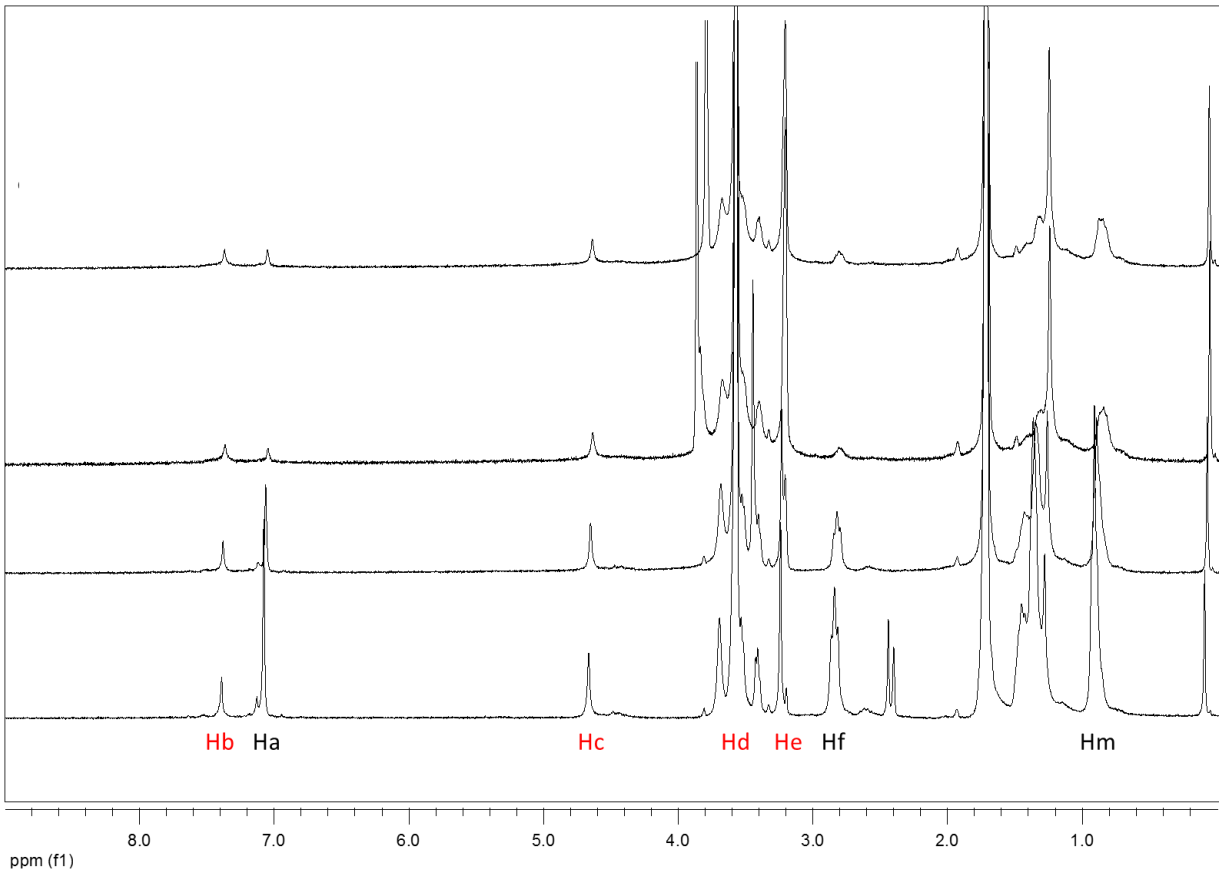

Figure S3. ^{1}H NMR of P3HT-*b*-P3TEGT (2mg/mL THF-d8) with successive addition of MeOD from bottom to top: 0 (a), 0.02 mL (b), 0.04 mL (c), 0.06 mL (d).

SI.2.2.2 Dynamic light scattering studies of P3HT-*b*-P3TEGT micelles

The stability and size distribution of P3HT-*b*-P3TEGT micelles were further characterized by DLS measurements. To examine the influence of the concentration of polymeric materials and solvent composition on the micelle stability, different types of micelle were studied consisting of three concentrations of P3HT-*b*-P3TEGT in THF/MeOH. All DLS measurements showed that the aggregates have monomodal size distribution (table S1). As expected, 1 mg/mL micelles show the best stability. In contrast low and high concentration of polymeric materials display less stable micelles. Thus for the concentration of 0.05 mg/mL and 1 mg/mL, the hydrodynamic diameter of the aggregates were found to be large 684 nm and 98 nm respectively, then stable micelles with a size of 160 ± 13 nm and 45 ± 4 nm respectively, were formed when the ratio of methanol increased from 50% to 100%. These results are in agreement with the absorption results. While for micelles formed using high concentration of P3HT-*b*-P3TEGT (5 mg/mL), the size of micelle is larger and variable, for low ratio of methanol, 30% the micelle has a size of 576 nm, and decrease with increasing the ratio of methanol till achieve 118 nm at 100 %.

Table S1. The average diameter of nanomicelles with different ratio of methanol measured by DLS

Methanol %	Size (d. nm) 0.05 mg/mL	1 mg/mL	5 mg/mL
30	684 ± 4	98 ± 4	576 ± 21
50	174 ± 4	47 ± 8	552 ± 13
70	161 ± 5	43 ± 4	325 ± 7
100	147 ± 3	41 ± 5	118 ± 9

SI. 3 Preparation and characterizations of electroactive bio-interface based on mannose-decorated P3HT-*b*-P3TEGT nanoparticles.

SI.3.1. Electrochemical characterization

SI.3.1.1 CV and EIS characterization of P3HT and P3HT-*b*-P3TEGT

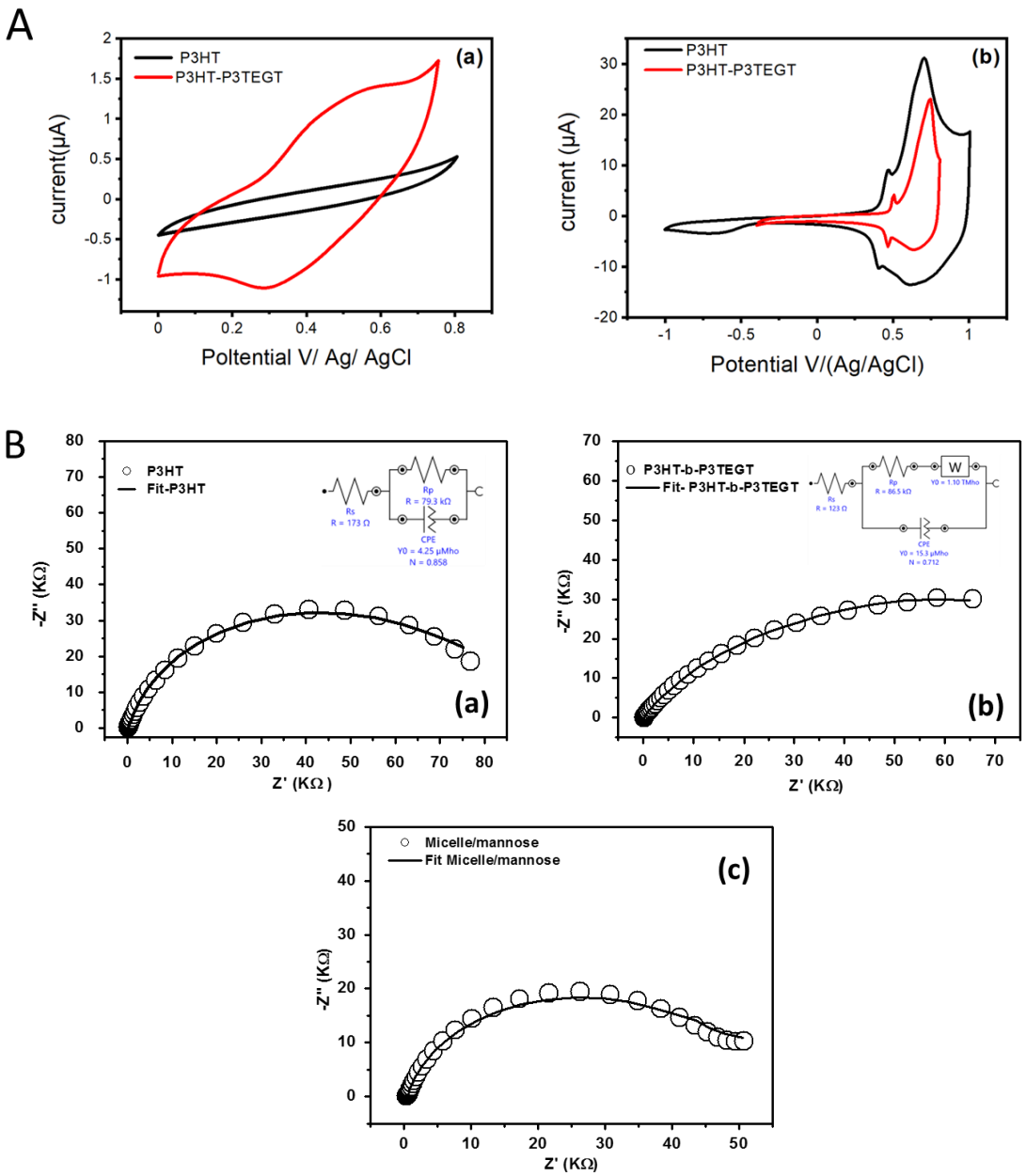

Figure S4. (A) CV curves in 10 mM PBS buffer pH 7.2 (a) and acetonitrile containing 0.1M $LiClO_4$ (b) performed at 50 mV/s for films of P3HT–*b*-P3TEGT/GCE and P3HT/GCE**, (B)** EIS of modified GCE P3HT/GCE (a) P3HT–*b*-P3TEGT/GCE (b), and nanomicelles of P3HT-*b*-P3TEGT/mannose (c) obtained at potential of -0.4V with DC of 10 mV and frequency range of 100 kHz to 0.1 Hz.

Table S2. Values obtained from equivalent circuit elements by fitting the EIS experimental data

Element	Rs (Ω)	Rct (KΩ)	C (µF)	N	W1	X^2
P3HT	172	79.2	4.2	0.85	----	0.019
P3HT-*b*-P3TEGT	123	86.5	15.3	0.71	1.10E+12	0.003
Nanomicelles/mannose	273	47	2.59	0.84	1.2 E+4	0.05

SI. 3.2 Bio-interface based on mannose-decorated P3HT-*b*-P3TEGT nanoparticles, formation and optimizations

The bio-interface is fabricated by coating mannose decorated nanoparticles solution on GCE. The obtained films have hydrophilic surface properties as proven by contact angle measurements. We noted that, during bacteria incubation some films partially detached from the electrode, or partially dissolved as well when the mannose is entrapped. Thus, the condition of the bio-interface formation as well as the film coating were optimized in order to improve the adhesion of the film and to avoid its detachment from electrode or its dissolution during the incubation with bacteria. To control the stability of the film, EIS measurements were performed after dipping mannose-P3HT-*b*-P3TEGT modified electrodes in PBS solution during 1 to 4 h. The modifications of EIS signals of mannose-P3HT-*b*-P3TEGT modified electrode, inform on the stability of the layer. Indeed, each surface modification such as detachment of the film, partially dissolution of the mannose should modify the EIS signal. Firstly, the condition of film formation was investigated by the examination of the effect of time and temperature annealing of the bio-interface. When the film is dried at room temperature EIS signal shows a decrease of impedance after 1h incubation in PBS (Figure S5 a). This result demonstrates a loss of the electroactivity of the film due to the partial dissolution or detachment of the film. Then, the annealing temperature was selected to 50 °C, which allows the evaporation of the solvent without damaging the film and formation of the cracks. The optimization of the annealing times was achieved and EIS signal was recorded for mannose/P3HT-*b*-P3TEGT films annealed at 50°C after different times 30 min, 60 min and 120 min. The modified electrodes were then incubated in PBS solution at various times 1h, 2h, 3 h and 4h and EIS measurements were recorded after each incubation time for each electrode. The results showed that annealing the mannose/P3HT-b-P3TEGT modified electrode for 30 min or 1 h at 50 °C gives unstable EIS signal after immersing the film on PBS

buffer for 1 h (figure S5, curve b and c). However, extend the annealing time to 2 h gives stable EIS responses after increasing time periods of incubation from 1h to 4h (figure S5 curve d). This demonstrates that the quality of adhesion of the film on the electrode is improved with the temperature and annealing time of 2h.

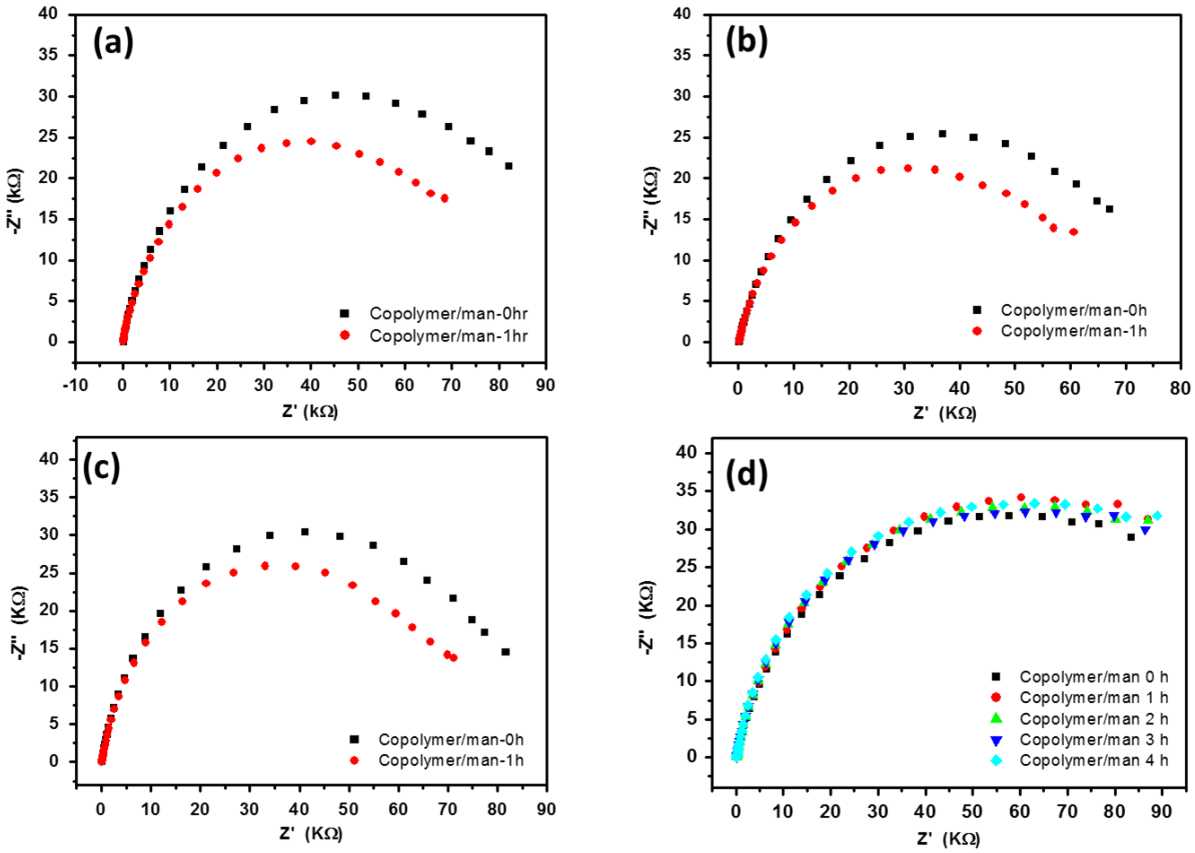

Figure S5. EIS measurements of mannose/P3HT-b-P3TEGT modified electrode in PBS solution, with different annealing times: a) without annealing, (b) annealed at 50 ^{0}C for 30 min, (c) annealed at 50 ^{0}C for 1 h and (d) annealed at 50 ^{0}C for 2 h.

SI. 4 Bacteria detection

SI.4.1 EIS characterization of mannose/P3HT-*b*-P3TEGT modified electrodes for bacteria detection

The sensitivity of mannose/P3HT-*b*-P3TEGT bio-interface towards various concentrations of *E. coli* bacteria was studied using different ratios of mannose: P3HT-*b*-P3TEG nanoparticles. The ratio of mannose: P3HT-*b*-P3TEG nanoparticles was optimized through different volume ratios of micelle solution added to the mannose-methanol solution. EIS measurements were performed after the incubation with different concentrations of *E.coli*

bacteria (Figure S6) and calibration curves were plotted by measuring the relative variation of Rct with *E. coli* concentration present during the incubation. The results show that film coated with P3HT-*b*-P3TEGT: mannose in mass ratio of 1:5 (P1M5) provides non-linear detection regarding the concentration of *E. coli* (Figure S6A). This non-linearity observed at high concentration, where the EIS shows a decrease of the response, can be explained by a loss of a small amount of mannose which is not entrapped in P3HT-b-P3TEG structure or the top surface of the film is rich in mannose, which in high concentration of *E. coli* cells leads to detachment and/or dissolution of the mannose from the surface. The film fabricated with the mass ratio 2:5 (P2M5) shows linear variation of EIS with the concentration of *E. coli* with wide dynamic range from 10^3 CFU/mL to 10^7 CFU/ml, as shown in Figure 9 in manuscript. This ratio provides more homogenous surface with sufficient stabilized mannose in P3HT-*b*-P3TEG structure. Results from the fitting of impedance data with different concentration of *E. coli* are summarized in (Table S3).

Table S3: EIS parameters for various concentration of bacteria detection

***E. coli* (CFU/mL)**	**Rs (Ω)**	**Rct (KΩ)**	**CPE (µF)**	**N**	**W1**	**X^2**
0	282.4	44.5	2.38	0.86	0.00010873	0.06
10^3	266.62	50.3	2.98	0.83	0.0001034	0.01
10^4	274.01	56.4	3.83	0.80	8.2837E-05	0.01
10^5	266.28	64.9	2.97	0.83	8.3394E-05	0.03
10^6	294.22	68.6	3.73	0.83	9.0302E-05	0.05
10^7	200.65	73.2	3.31	0.82	7.5701E-05	0.04

The bio-interface fabricated with ratio 3:5 of P3HT-*b*-P3TEGT: mannose (P3M5) with high concentration of polymer gives limited detection range from (10^3 CFU/mL to 10^4 CFU/mL followed by saturation as seen in Figure S6 B. This is due to a low amount of mannose decorated the nano-micelles where saturation was reached rapidly.

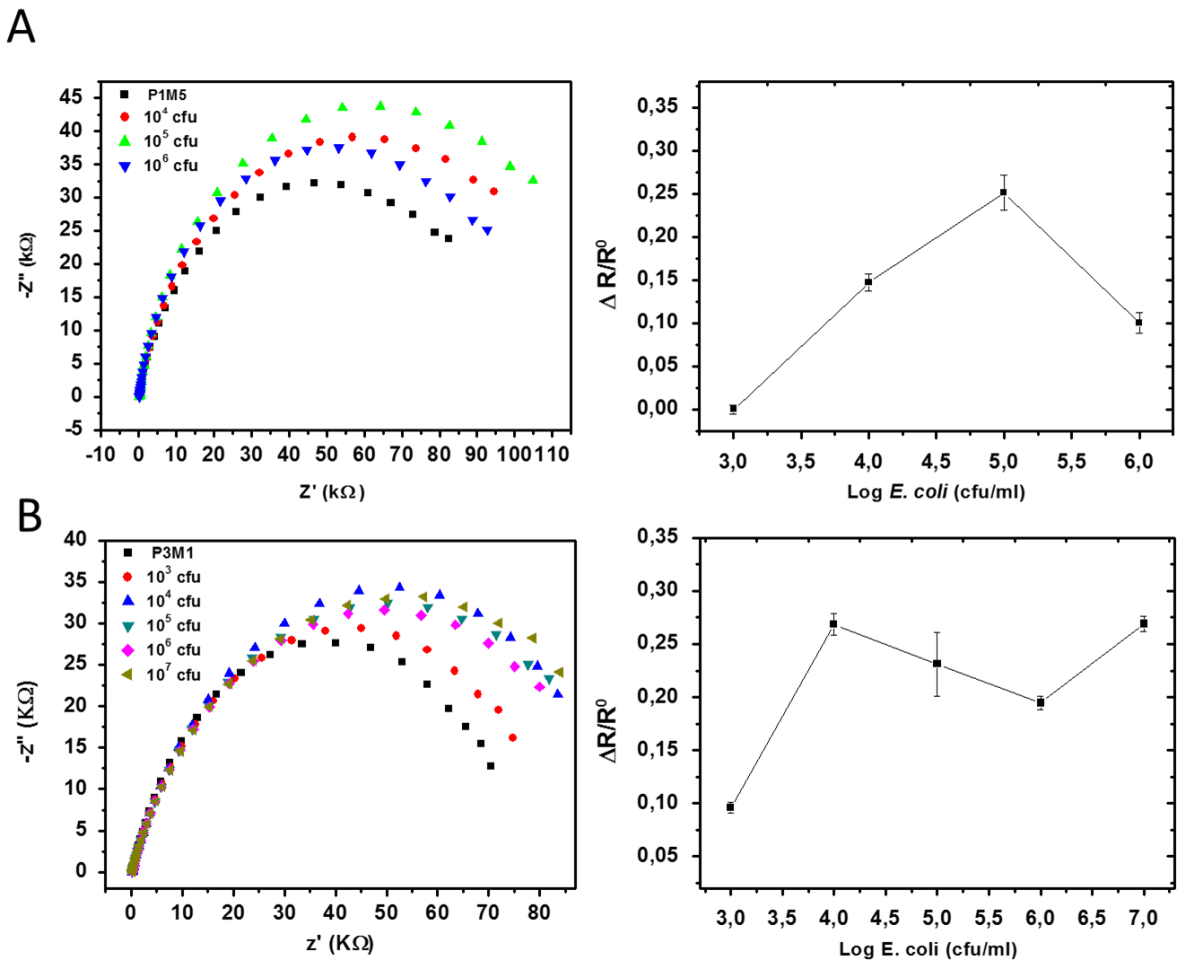

Figure S6. EIS Nyquist diagrams of a GCE modified with P3HT-b-P3TEGT/mannose (left) and calibration curve obtained from the average variation of Rct with different concentrations of *E. coli (right)*, the parameters varied is the mass ratio copolymer: mannose; (1:5, P1M5) (A) and (3:5, P3M5) (B).

Table S4. Comparison of electrochemical sensing of bacteria using conjugated polymers as electrode material(PANI :polyaniline, Glu: glutaraldehyde; PDOT:PSS: poly(3,4-ethylenedioxythiophene):polystyrenesulfonate; EET: Extracellular electron transfer; dVt: potentiometric)

Bacteria	Transducers	Detection	Sensing method	LOD CFU/mL	Linear range CFU/mL	ref
Salmonella typhimurium	poly(pyrrole-co-3-carboxyl-pyrrole)/aptamer conjugate	direct	EIS	3	10^2 to 10^8	1
E. coli O86 coli W1485	P3 (thiophene-3-quinone)/mannose	direct	SWV	800	$2\ 10^3$ - 10^4	2
Salmonella	PEDOT:PSS	Indirect EET	dVt	$6.6\ 10^6$	NA	3
E. coli O157:H7 (purified)	PANI/Glu/antibody	Purification step	ESI	100	$10\text{-}10^7$	4
E. Coli	P3HT-*b*-P3TEGT/mannose	direct	EIS	500	10^3- 10^7	This work

SI.4. 2 Analysis of Nile River samples

To evaluate the sensor performance on real environmental water sample, sample of untreated Nile River was measured by our proposed technique in comparison with colony counting method through conventional culture by making five serial dilutions of untreated water sample and plating 100 µL of each dilution on appropriate agar plates. After overnight incubation of agar plates, the following formula was applied:

Cells/mL (CFU/mL) = number of colonies counted * dilution factor * 10.

EIS signal of sensor was measured using filtered sample as blank (no bacteria) and untreated Nile river sample after incubation for 1 h. The signal produced an average variation of Rct ($\Delta R/R^0 = 0.359$) when reported to calibration curve gives the value of $\approx 10^6$ CFU/mL of Bacteria. On the other side, the result from conventional counting method after serial dilution was $5.6x10^5$ CFU/mL.

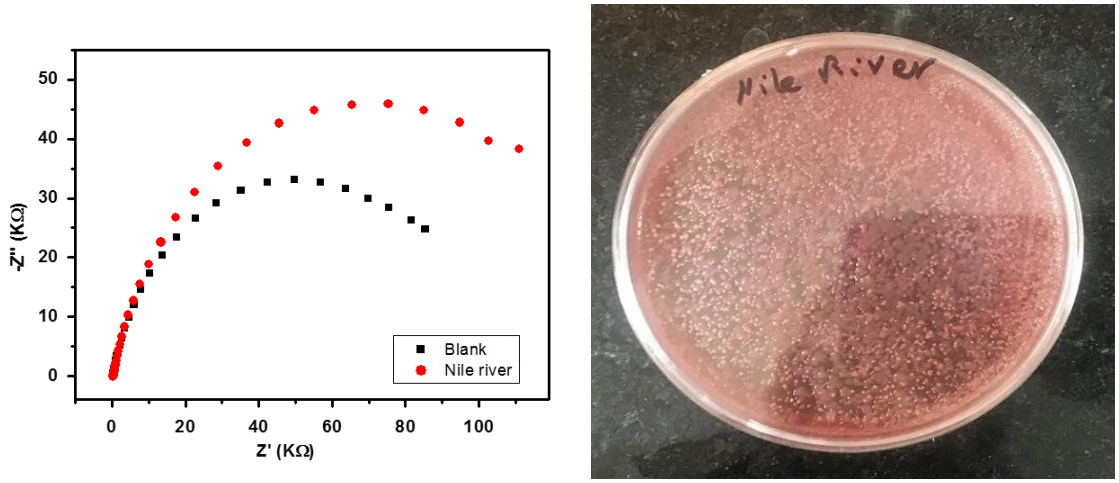

Figure S7. EIS signal produced from Nile River sample, black curve is the blank test with the sample filtered and red curve is sample non filtered (a), conventional plate culture for 100 µL of untreated Nile River sample on Macconkey agar media (b).

References

(1) Sheikhzadeh, E.; Chamsaz, M.; Turner, A. P. F.; Jager, E. W.H.; Beni, V. Biosens. Bioelectron. **2016**, 80, 194−200.

(2) Ma, F.; Rehman, A.; Liu, H. Y.; Zhang, J. T.; Zhu, S. L.; Zeng, X. Q. Anal. Chem. **2015**, 87, 1560−1568.

(3)Butina, K.; Löfflera, S.; Rhenb, M.; Richter-Dahlfor, A. Sens. Act.: B. Chem. **2019**, 297 , 126703

(4)Chowdhury, A. D; . De, A.;. Chaudhuri, C. R.; Bandyopadhyay, K.; Sen, P. Sens. Act.: B. Chem. **2012**, 171-172, 916-923